Journal of Materials Chemistry A

Electronic Supplementary Information

The effect of thermal history on oxygen surface exchange on $(La_{0.6}Sr_{0.4})_{0.99}CoO_{3-\delta}$ and $(La_{0.6}Sr_{0.4})_{0.98}FeO_{3-\delta}$

Đorđije Tripković, Rainer Küngas, Mogens Bjerg Mogensen, Peter Vang Hendriksen

Electrical conductivity relaxation

The electrical conductivity (σ) of LSC and LSF directly depends on the internal defect equilibrium which is correlated with the concentration of oxygen ions. This in turn depends on temperature and oxygen activity in the surrounding atmosphere. Hence, a sudden change in oxygen activity around the material will affect the conductivity. The rate at which the sample equilibrates with the new atmosphere depends on oxygen mobility in the sample and the rate of the oxygen exchange over the surface. This is what is exploited in a conductivity relaxation (ECR) experiment - it enables determination of surface exchange coefficient (k_{chem}) and bulk chemical diffusion coefficient (D_{chem}) from conductivity trend-line after an abrupt change in pO_2. Obtaining the oxygen transport parameters from the experimental data consists of fitting the measured conductivity trends with diffusion model by choosing optimal k_{chem} and D_{chem} values for a geometrically well-defined piece of material.[1–7] The diffusion model is given by Crank[8], based on the solution by Carslaw and Jaeger[9]:

$$\frac{\sigma_\infty - \sigma_t}{\sigma_\infty - \sigma_0} = \sum_{p=1}^{\infty} \frac{2L_x^2 \cdot \exp\left(\frac{-\beta_{p,x}^2 D_{chem} t}{a}\right)}{\beta_{p,x}^2\left(\beta_{p,x}^2 + L_x^2 + L_x\right)} \times \sum_{q=1}^{\infty} \frac{2L_y^2 \cdot \exp\left(\frac{-\beta_{q,y}^2 D_{chem} t}{b}\right)}{\beta_{q,y}^2\left(\beta_{q,y}^2 + L_y^2 + L_y\right)} \times \sum_{r=1}^{\infty} \frac{2L_z^2 \cdot \exp\left(\frac{-\beta_{r,z}^2 D_{chem} t}{c}\right)}{\beta_{r,z}^2\left(\beta_{r,z}^2 + L_z^2 + L_z\right)} \quad (SE.1)$$

Here σ_0, σ_∞, and σ_t represent conductivity at the start, at the end, and at a particular time in the experiment, respectively. Subscripts x, y, and z indicate the three dimensions and a, b, and c, stand for halves of width, length and height of a rectangular sample. These are used for calculating the respective dimensionless parameters:

$$L_x = \frac{a \cdot k_{chem}}{D_{chem}} \quad (SE.2)$$

$$L_y = \frac{b \cdot k_{chem}}{D_{chem}} \quad (SE.3)$$

$$L_z = \frac{c \cdot k_{chem}}{D_{chem}} \quad (SE.4)$$

βs are the positive roots of the respective equations:

$$\beta_{p,x} \cdot \tan \beta_{p,x} = L_x \quad (SE.5)$$

$$\beta_{q,y} \cdot \tan \beta_{q,y} = L_y \quad (SE.6)$$

$$\beta_{r,z} \cdot \tan \beta_{r,z} = L_z \quad (SE.7)$$

If one of the samples dimensions is much larger than the others (e.g. $a \gg b, c$), then the diffusion along that dimension can be neglected which can simplify the equation SE.1 to a 2D or 1D expression. The dimensionless parameter L (eq. SE.1-3) directly determines the sensitivity of the response to k_{chem} and D_{chem} and thus the accuracy with which these can be determined. If L is large then the estimation of k_{chem} becomes difficult and the measurement is said to be in diffusion-controlled regime. On the other hand, small L means more difficult estimation of D_{chem} and a surface-controlled regime. For intermediate values, $0.03 \ll L \ll 30$ [10], the measurement is in mixed-control regime and both k_{chem} and D_{chem} can be determined accurately.

Supporting figures

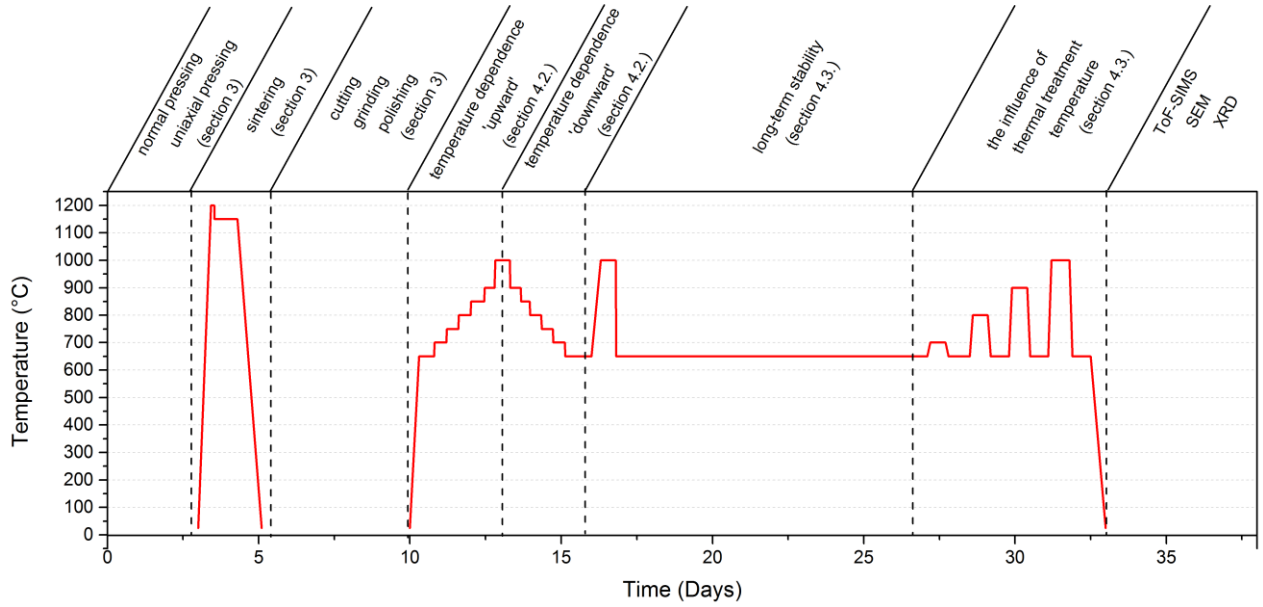

S1. A sketch depicting thermal history of the samples investigated in this study and the experimental sequence

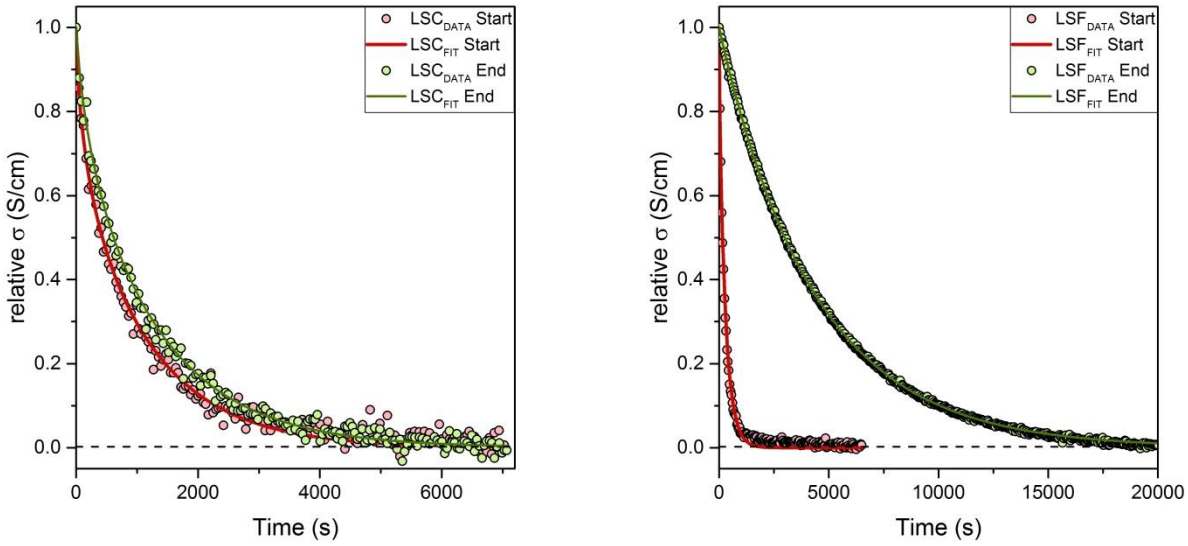

S2. Conductivity relaxation curves for LSC (left) and LSF (right) 5 hours after the thermal treatment at 1000°C and after 10 days at 650°C. Note: only 2% of all measured points are plotted due to readability

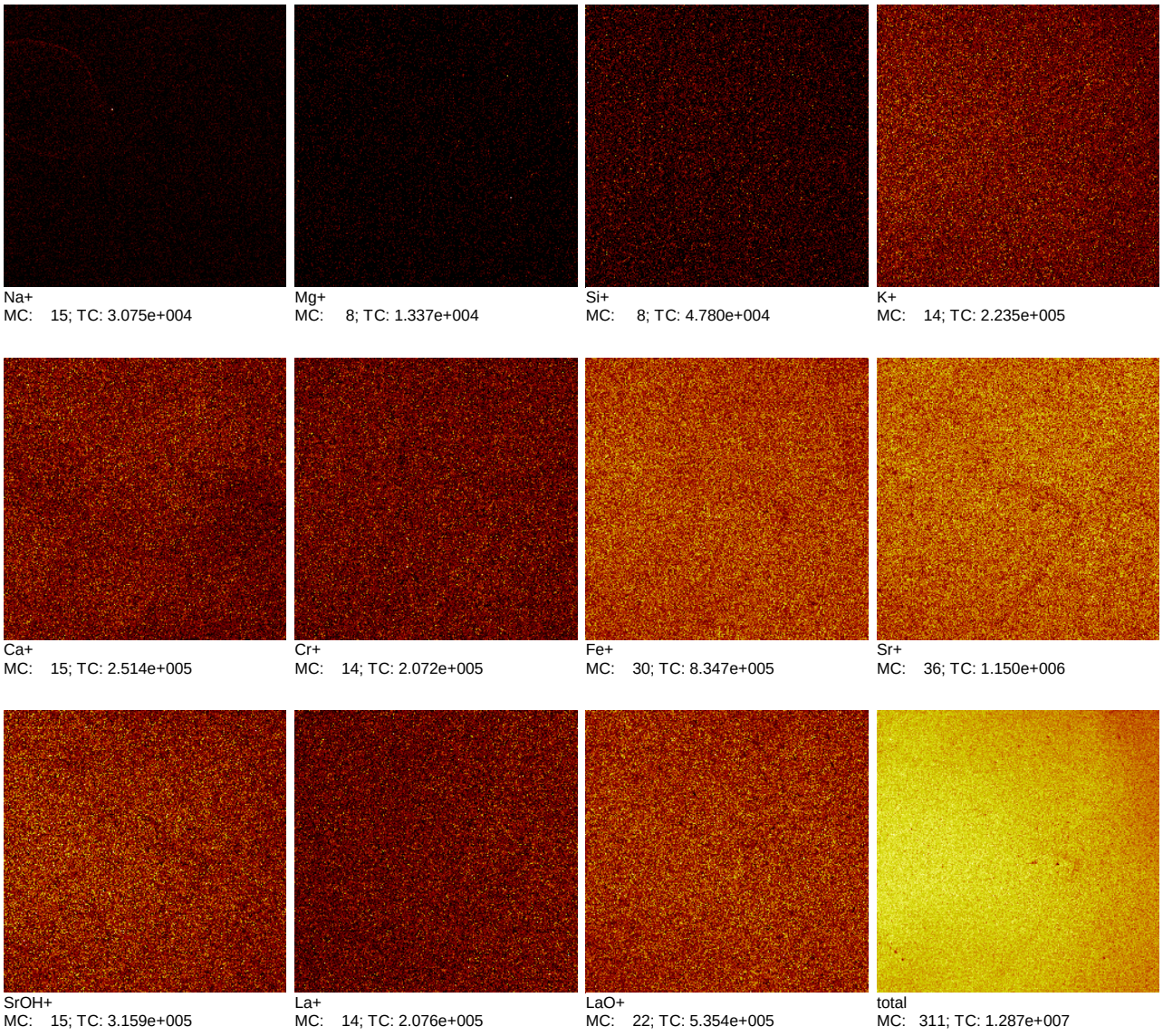

S3. ToF-SIMS imaging of LSF after the ECR measurement – square size 500 µm x 500 µm

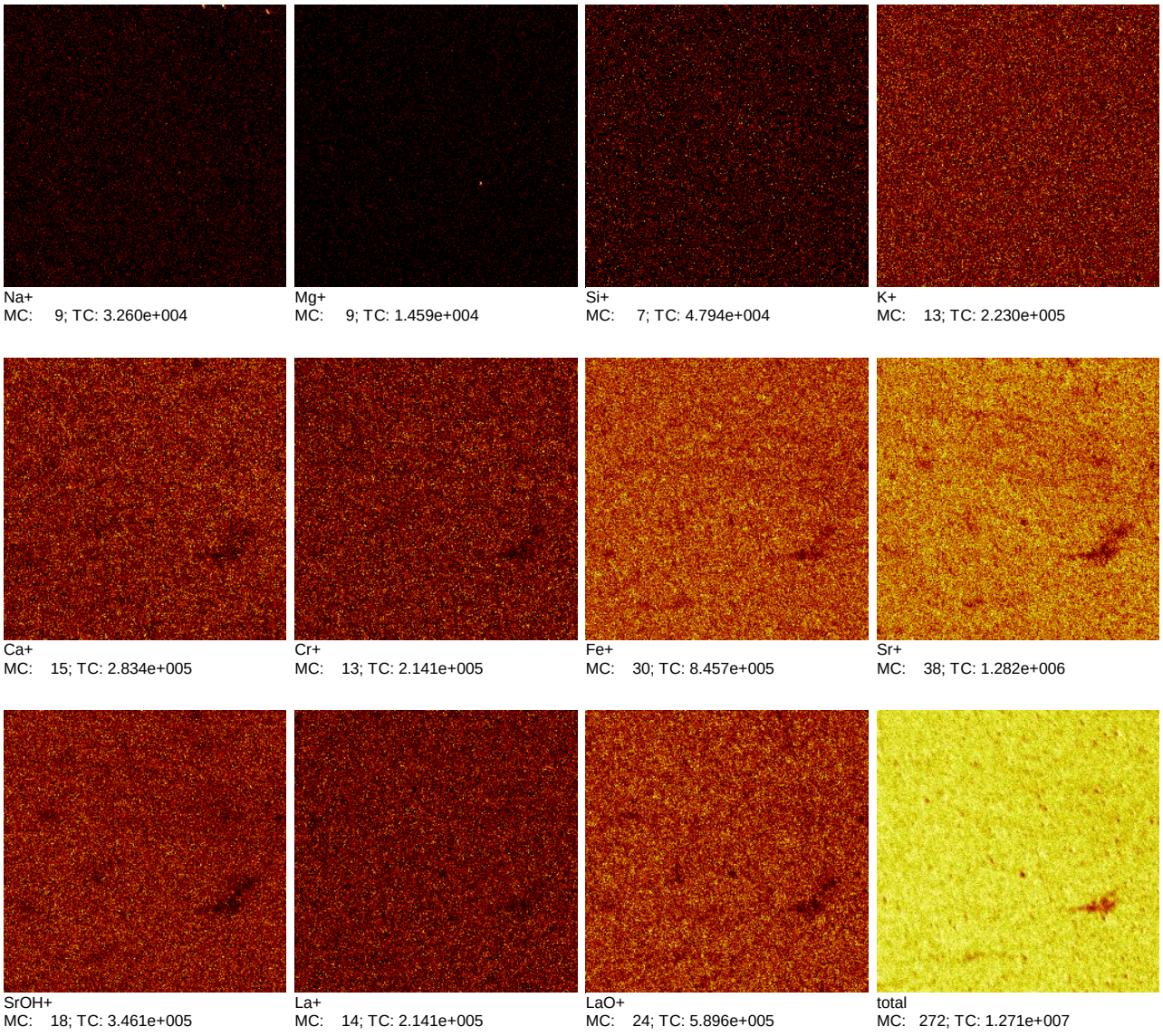

S4. ToF-SIMS imaging of LSF after the ECR measurement – square size 100 µm x 100 µm

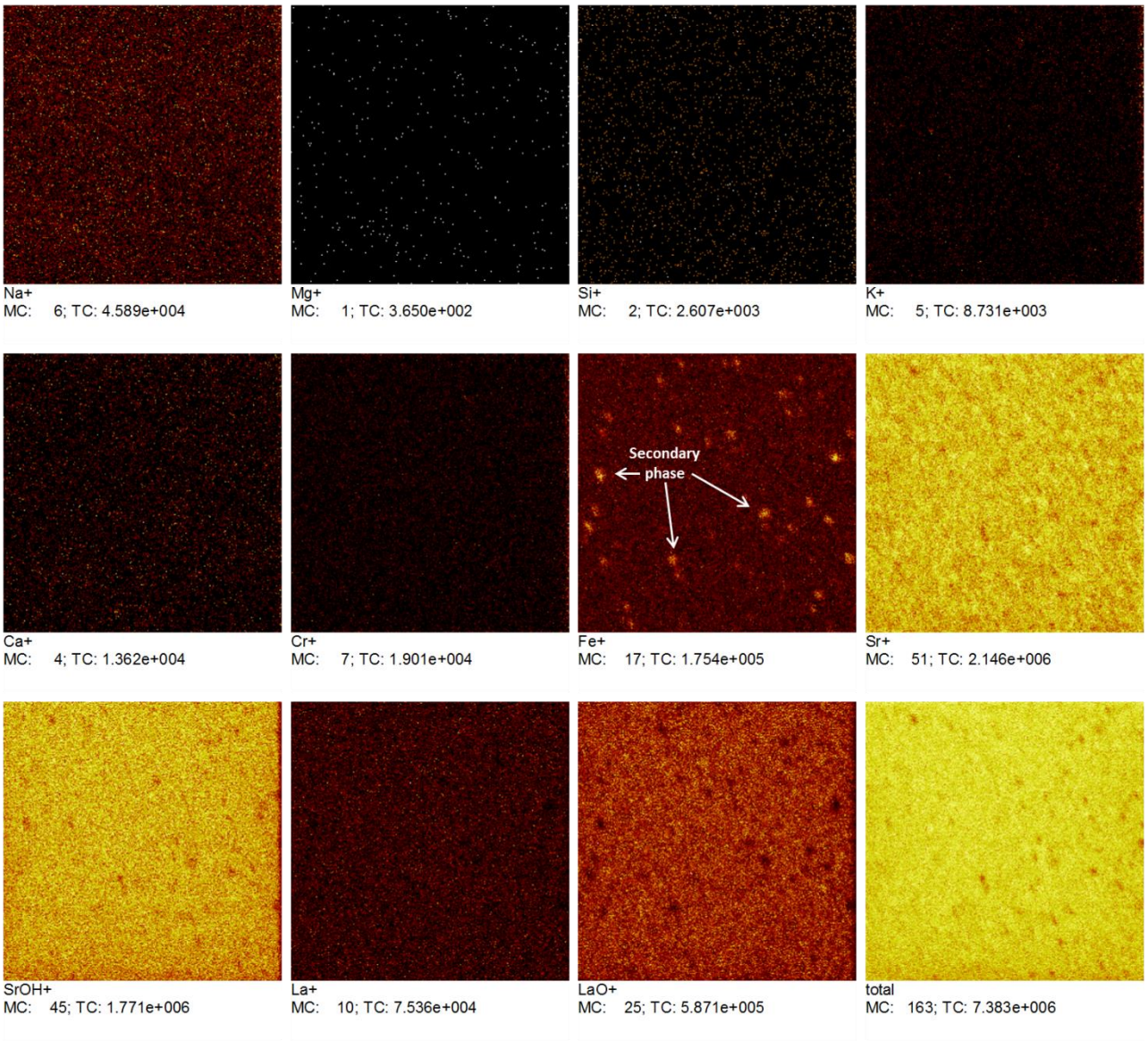

S5. ToF-SIMS imaging of LSF after the ECR measurement – square size 50 µm x 50 µm

S6. Results of ICP analysis of LSF powder

Ions	**Atomic content %**
Fe	50.674±0.018
La	29.437±0.179
Sr	19.673±0.125
K	0.127±0.035
Na	0.049±0.005
Li	0.040±0.006
La+Sr+Fe	99.784±0.107
Impurities	0.216±0.015

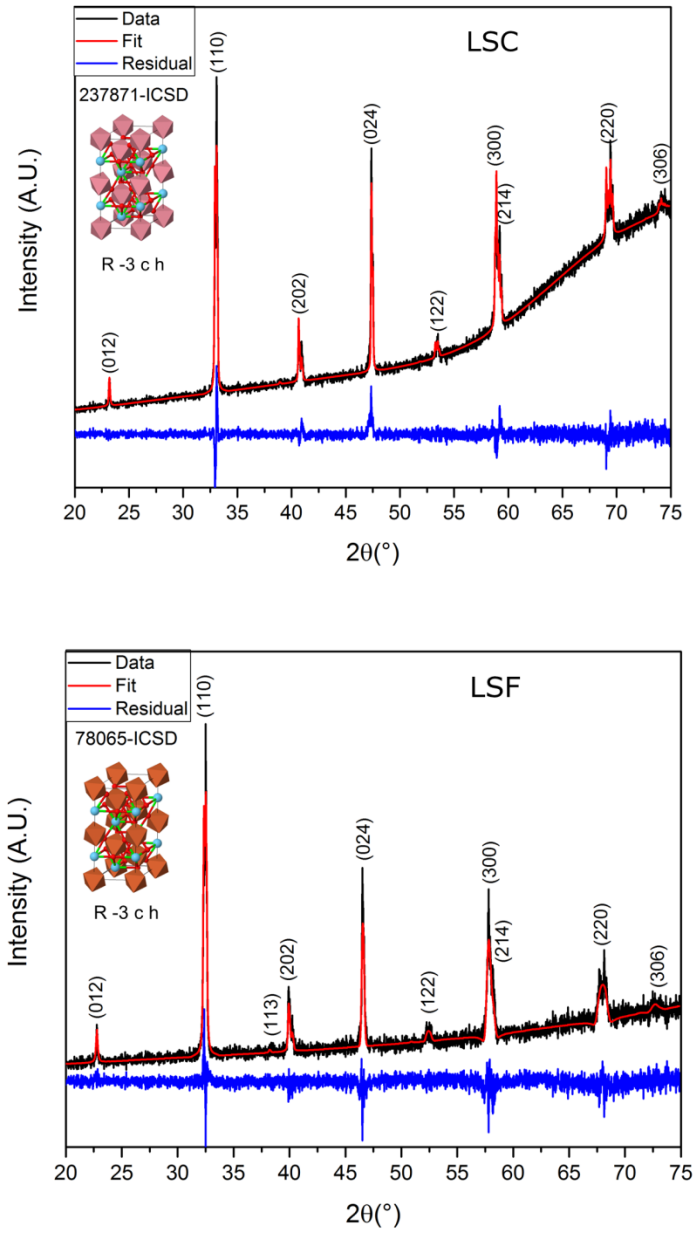

S7. Rietveld refined XRD diffractograms of LSC (up) and LSF (down)

S8. Unit cell parameters based on Rietveld refinement for LSC and LSF

Parameter	*LSC*	*LSF*
a	5.4361 Å	5.5307 Å
b	5.4361 Å	5.5306 Å
c	13.2205 Å	13.4355 Å
α	90°	90°
β	90°	90°
γ	120°	120°

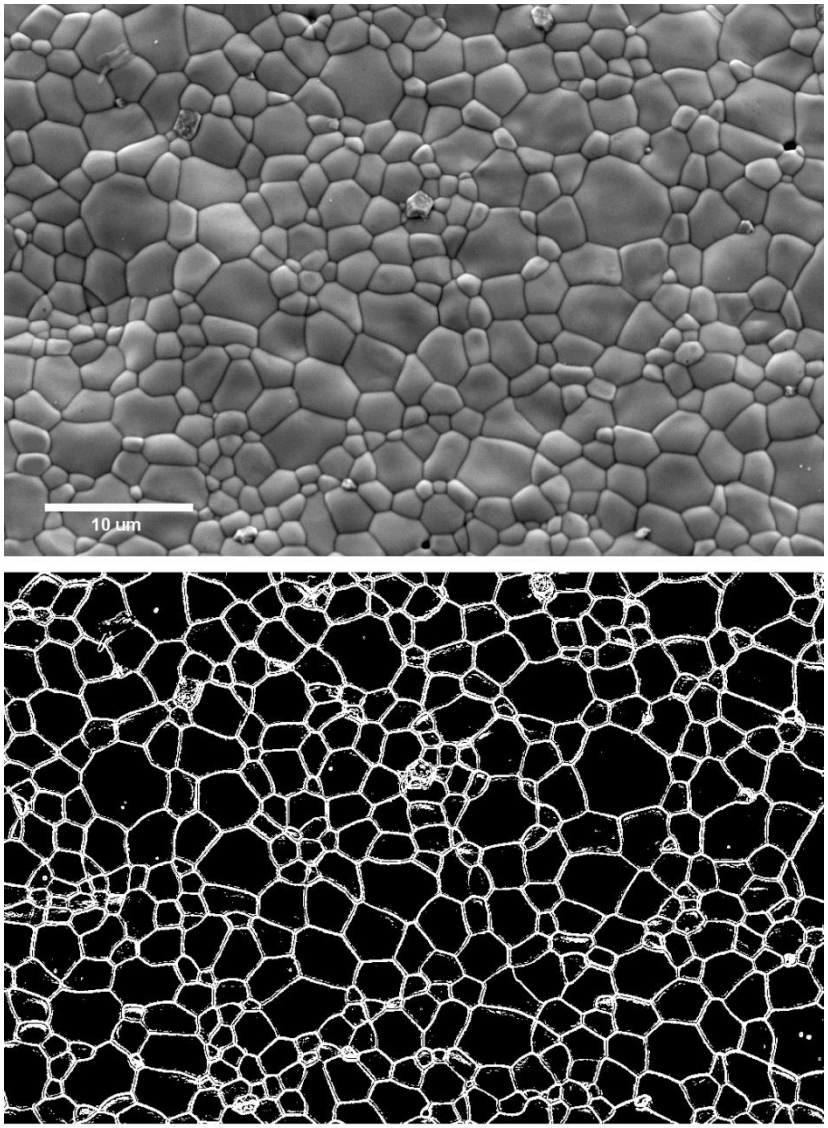

S9. SEM of LSC surface and grain-size estimation after the ECR measurement

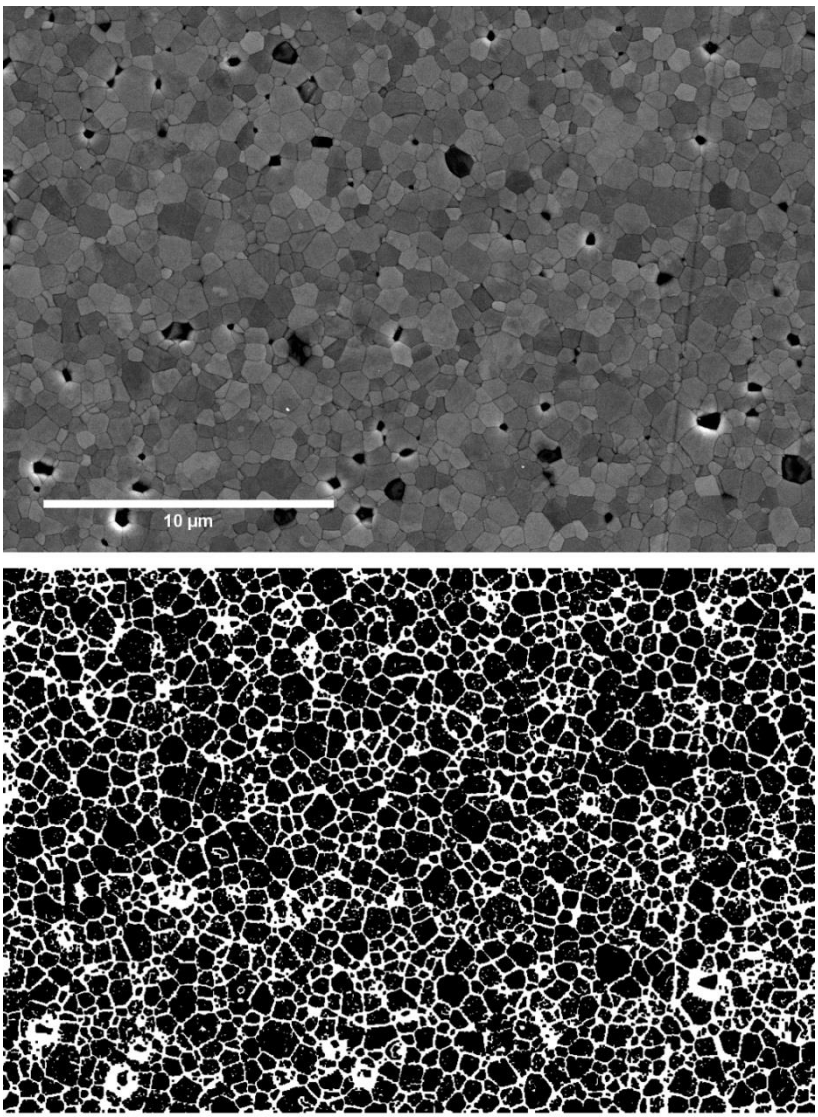

S10. SEM of LSF surface and grain-size estimation after the ECR measurement

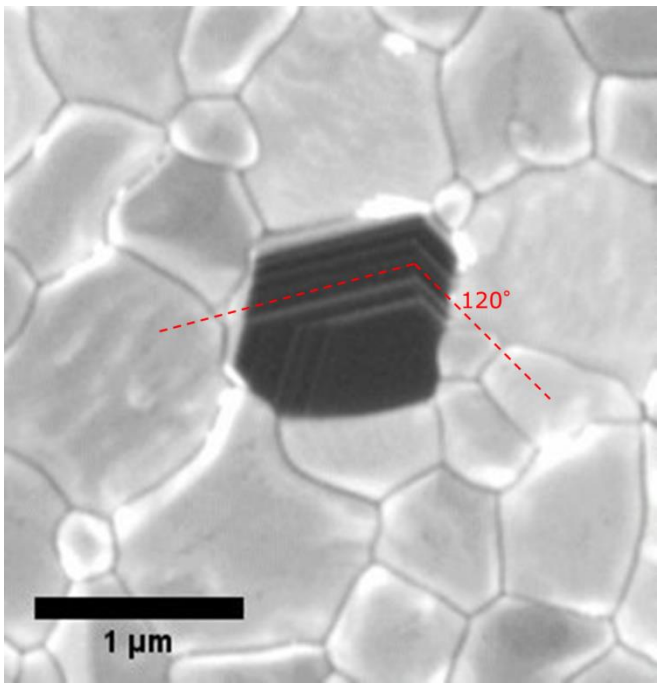

S11. Secondary phase in LSF

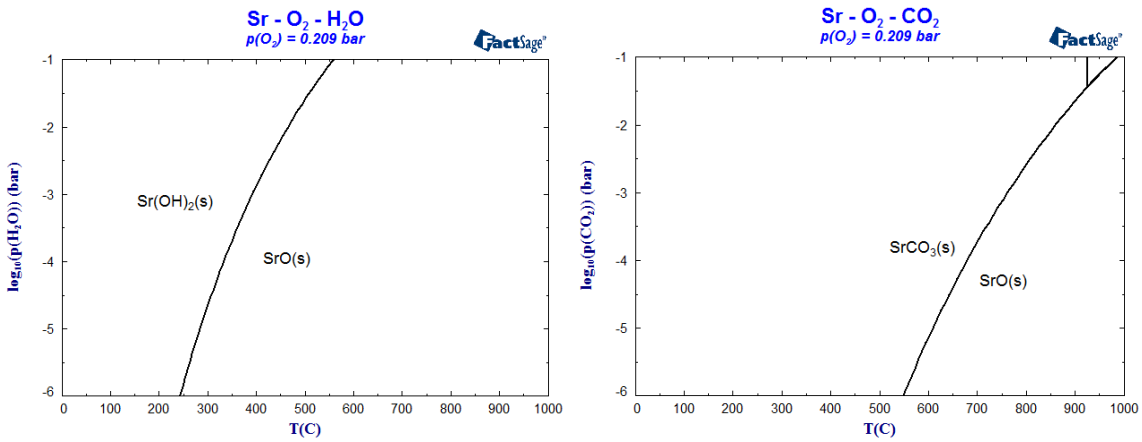

S12. Phase diagrams showing the stability of strontium hydroxide and carbonate

References

1 I. Yasuda, *J. Electrochem. Soc.*, 1994, **141**, 1268.

2 I. Yasuda and M. Hishinuma, *Solid State Ionics*, 1995, **80**, 141–150.

3 I. Yasuda and M. Hishinuma, *J. Solid State Chem.*, 1995, 115, 152–157.

4 I. Yasuda and M. Hishinuma, *J. Solid State Chem.*, 1996, **123**, 382–390.

5 J. A. Lane and J. A. Kilner, *Solid State Ionics*, 2000, **136–137**, 997–1001.

6 J. E. ten Elshof, M. H. R. Lankhorst and H. J. M. Bouwmeester, *J. Electrochem. Soc.*, 1997, **144**, 1060.

7 M. Søgaard, P. V. Hendriksen, M. Mogensen, F. Poulsen and E. Skou, *Solid State Ionics*, 2006, **177**, 3285–3296.

8 J. Crank, *Oxford Univ. Press*, 1975, 414.

9 H. S. Carslaw, J. C. Jaeger and H. Feshbach, *Phys. Today*, 1962, **15**, 74–76.

10 M. W. den Otter, H. J. M. Bouwmeester, B. A. Boukamp and H. Verweij, *J. Electrochem. Soc.*, 2001, **148**, J1.